CHEMISTRY OF MATERIALS

Article

Quantum Dots from Chemical Aerosol Flow Synthesis: Preparation, Characterization, and Cellular Imaging

Jin Ho Bang, Won Hyuk Suh, and Kenneth S. Suslick

Chem. Mater., **2008**, 20 (12), 4033-4038 • DOI: 10.1021/cm800453t • Publication Date (Web): 30 May 2008

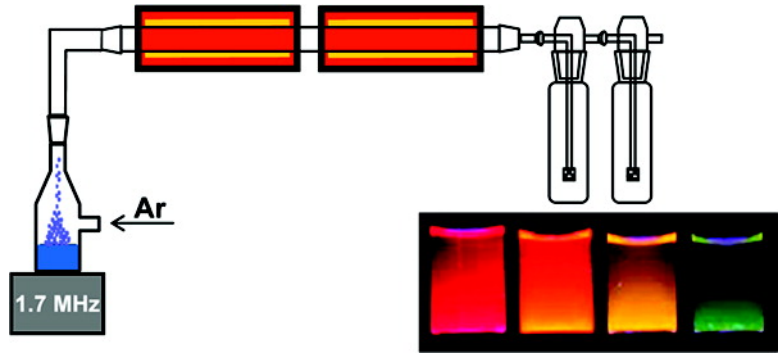

More About This Article

Additional resources and features associated with this article are available within the HTML version:

- Supporting Information
- Access to high resolution figures
- Links to articles and content related to this article
- Copyright permission to reproduce figures and/or text from this article

View the Full Text HTML

Chemistry of Materials is published by the American Chemical Society. 1155 Sixteenth Street N.W., Washington, DC 20036

Quantum Dots from Chemical Aerosol Flow Synthesis: Preparation, Characterization, and Cellular Imaging

Jin Ho Bang, Won Hyuk Suh, and Kenneth S. Suslick*

School of Chemical Sciences, University of Illinois at Urbana−Champaign, 600 South Mathews Avenue, Urbana, Illinois 61801

Received February 14, 2008. Revised Manuscript Received April 9, 2008

CdTeSe and CdTeS ternary quantum dots (QDs) that fluoresce in the red to near-IR regions have been prepared using chemical aerosol flow synthesis (CAFS). Changing the composition ratio of Te to Se permits bandgap tuning of CdTeSe QDs, and replacing selenium with sulfur in the precursor solution increased the quantum efficiency of CdTe QDs up to ∼37%, because of better surface passivation of the CdS outer shell that grows on top of the CdTe core. ICP-MS and XPS analyses showed the internal structure of these ternary QDs had a gradient in the Se/Te concentration ratio with a CdTe-rich core. A simple phase transfer reaction rendered CdTeSe QDs water-soluble, and the water-soluble CdTeSe QDs were evaluated as a fluorescence labeling agent for intracellular imaging applications. A blue shift in the photoluminescence of CdTeSe QDs was observed over time both in living cells and in solutions under air exposed to light, which is attributed to photo-oxidation of the outer shell.

Introduction

In recent years, the unique size- and shape-dependent optical and electronic properties of semiconductor nanocrystals (or quantum dots, QDs) found increased use in diverse applications, including lasers, light-emitting devices, biological imaging, and photovoltaics.[1–10] Cadmium-based chalcogenide nanoparticles have received extensive examination in many fields because of their size- and composition-dependent bandgap tunability.[11–17] There have been several synthetic methods developed for nanoparticle synthesis: coprecipitation in solution,[18–21] high-temperature decomposition of organometallic precursors,[22–25] microwave-assisted synthesis,[26–28] hydrothermal synthesis,[29] and sonochemical synthesis.[30,31] The most successful synthetic route involves the rapid injection of molecular precursors into heated organic solvents containing surfactants,[22–25] which separates the nucleation and growth periods of nanoparticles by simply controlling temperature and results in highly crystalline nanoparticles with narrow size distributions.[32,33] It remains a significant challenge, however, to scale up this synthesis because of its requirement of rapid nucleation through thermal or concentration spikes.[34–37] Chemical aerosol flow synthesis (CAFS), which uses ultrasonic nebulization and

* Corresponding author. E-mail: ksuslick@uiuc.edu.

(1) Huynh, W. U.; Dittmer, J. J.; Alivisatos, A. P. *Science* **2002**, *295*, 2425.
(2) Colvin, V. L.; Schlamp, M. C.; Alivisatos, A. P. *Nature* **1994**, *370*, 354.
(3) Bruchez, M.; Moronne, M.; Gin, P.; Weiss, S.; Alivisatos, A. P. *Science* **1998**, *281*, 2013.
(4) Chan, W. C. W.; Nie, S. *Science* **1998**, *281*, 2016.
(5) Klimov, V. I.; Mikhailovsky, A. A.; Xu, S.; Malko, A.; Hollingsworth, J. A.; Leatherdale, C. A.; Eisler, H.-J.; Bawendi, M. G. *Science* **2000**, *290*, 314.
(6) Coe, S.; Woo, W.-K.; Bawendi, M.; Bulović, V. *Nature* **2002**, *420*, 800.
(7) Dubertret, B.; Skourides, P.; Norris, D. J.; Noireaux, V.; Brivanlou, A. H.; Libchaber, A. *Science* **2002**, *298*, 1759.
(8) Tessler, N.; Medvedev, V.; Kazes, M.; Kan, S.; Banin, U. *Science* **2002**, *295*, 1506.
(9) Zhao, J.; Bardecker, J. A.; Munro, A. M.; Liu, M. S.; Niu, Y.; Ding, I.-K.; Luo, J.; Chen, B.; Jen, A. K.-Y.; Ginger, D. S. *Nano. Lett.* **2006**, *6*, 463.
(10) Gur, I.; Fromer, N. A.; Geier, M. L.; Alivisatos, A. P. *Science* **2005**, *310*, 462.
(11) Murray, C. B.; Kagan, C. R.; Bawendi, M. G. *Annu. Rev. Mater. Sci.* **2000**, *30*, 545.
(12) Peng, X.; Manna, L.; Yang, W.; Wickham, J.; Scher, E.; Kadavanich, A.; Alivisatos, A. P. *Nature* **2000**, *404*, 59.
(13) Manna, L.; Milliron, D. J.; Meisel, A.; Scher, E. C.; Alivisatos, A. P. *Nat. Mater.* **2003**, *2*, 382.
(14) Bailey, R. E.; Nie, S. *J. Am. Chem. Soc.* **2003**, *125*, 7100.
(15) Kim, S.; Fisher, B.; Eisler, H.; Bawendi, M. *J. Am. Chem. Soc.* **2003**, *125*, 11466.
(16) Zhong, X.; Feng, Y.; Knoll, W.; Han, M. *J. Am. Chem. Soc.* **2003**, *125*, 13559.
(17) Zhong, X.; Han, M.; Dong, Z.; White, T. J.; Knoll, W. *J. Am. Chem. Soc.* **2003**, *125*, 8589.
(18) Talapin, D. V.; Haubold, S.; Rogach, A. L.; Kornowski, A.; Haase, M.; Weller, H. *J. Phys. Chem. B* **2001**, *105*, 2260.
(19) Gaponik, N.; Talapin, D. V.; Rogach, A. L.; Hoppe, K.; Shevchenko, E. V.; Kornowski, A.; Eychmuller, A.; Weller, H. *J. Phys. Chem. B* **2002**, *106*, 7177.
(20) Zheng, Y.; Gao, S.; Ying, J. Y. *Adv. Mater.* **2007**, *19*, 376.
(21) Zheng, Y.; Yang, Z.; Ying, J. Y. *Adv. Mater.* **2007**, *19*, 1475.
(22) Murray, C. B.; Norris, D. J.; Bawendi, M. G. *J. Am. Chem. Soc.* **1993**, *115*, 8706.
(23) Peng, Z. A.; Peng, X. *J. Am. Chem. Soc.* **2001**, *123*, 183.
(24) Qu, L.; Peng, Z. A.; Peng, X. *Nano Lett.* **2001**, *1*, 333.
(25) Yu, W. W.; Peng, X. *Angew. Chem., Int. Ed.* **2002**, *41*, 2368.
(26) Gerbec, J. A.; Magana, D.; Washington, A.; Strouse, G. F. *J. Am. Chem. Soc.* **2005**, *127*, 15791.
(27) He, Y.; Sai, L.-M.; Lu, H.-T.; Hu, M.; Lai, W.-Y.; Fan, Q.-L.; Wang, L.-H.; Huang, W. *Chem. Mater.* **2007**, *19*, 359.
(28) Ziegler, J.; Merkulov, A.; Grabolle, M.; Resch-Genger, U.; Nann, T. *Langmuir* **2007**, *23*, 7751.
(29) Zhang, H.; Wang, L.; Xiong, H.; Hu, L.; Yang, B.; Li, W. *Adv. Mater.* **2003**, *15*, 1712.
(30) Murcia, M. J.; Shaw, D. L.; Woodruff, H.; Naumann, C. A.; Young, B. A.; Long, E. C. *Chem. Mater.* **2006**, *18*, 2219.
(31) Wang, C. L.; Zhang, H.; Zhang, J. H.; Li, M. J.; Sun, H. Z.; Yang, B. *J. Phys. Chem. C* **2007**, *111*, 2465.
(32) Peng, X.; Wickham, J.; Alivisatos, A. P. *J. Am. Chem. Soc.* **1998**, *120*, 5343.
(33) Peng, Z. A.; Peng, X. *J. Am. Chem. Soc.* **2002**, *124*, 3343.

10.1021/cm800453t CCC: $40.75
Published on Web 05/30/2008

reactive liquid droplets as the "microreactors", provides an important alternative methodology for continuous flow and simplicity of operation,[38] and we report here the extension of this work to ternary CdTeSe and CdTeS quantum dots.

CdTe QDs have received special attention because they can be widely tuned due to quantum confinement, and their emission can be extended to the near-infrared (NIR) wavelength region.[13,20,39–41] Far-red and near-IR (NIR) emitting QDs have the advantage that autofluorescence, light absorption, and scattering in biological systems are minimized in the NIR, providing a clear window for in vivo imaging.[14,15,41,42] In our previous report, we successfully synthesized CdTe nanocrystals stabilized by octadecylphosphonic acid (ODPA) with ~40% quantum efficiency;[38] the emission, however, could not be shifted further into the red than ~610 nm. The strong coordination bond in Cd-ODPA precursors significantly decreases the reactivity of the monomers,[39] and the residence time of aerosolized precursors during the flow synthesis was insufficient for CdTe QDs to grow to the large-sized particles necessary for far-red and NIR emission.[38]

Furthermore, it has been noted that the stability of the ODPA-stabilized CdTe QDs in air is relatively poor compared to the fatty-acid-coated QDs.[39] In this study, we have utilized oleic acid (OA) as a stabilizer to provide greater stability and have successfully extended the emission of CdTe QDs to the near-IR region using the CAFS method. Upon adding a third element (selenium) to the CdTe precursor solution and changing the reaction temperature, we were able to tune the emission wavelength of CdTe from red to near-IR. Further, the quantum efficiency of CdTe QDs was greatly improved by adding sulfur instead of selenium to the precursor solution because of better surface passivation of the CdS outer shell, which is grown during the flow synthesis over the initially formed CdTe core. Water-soluble CdTeSe QDs were prepared by a simple phase-transfer reaction and evaluated as a fluorescence labeling agent in live cell imaging. A blue shift in the photoluminescence of the QDs was observed both in living cells and in solution as previously noted,[43–46] and this blue shift is attributed to photo-oxidation.

Experimental Section

Synthesis of Cd-Based Ternary QDs. In a typical synthetic procedure, a mixture of cadmium oxide (1 mmol), oleic acid (4 mmol), and octadecene (5 mL) was heated to 250 °C under an Ar flow in a 50 mL three-necked flask until a clear solution was observed. The solution was then cooled to room temperature. TOPTe and TOPSe were prepared by adding tellurium (0.5 mmol) or selenium (3 mmol), respectively, to 2 mL of trioctylphosphine (TOP) and heating the mixture to 280 °C under argon gas flow. After cooling to room temperature, the TOPTe and TOPSe solutions were syringed into the prepared CdO solution, and toluene was then added to dilute the precursor solution to a total volume of 50 mL. The precursor solution was carefully transferred to the CAFS rig and nebulized by a 1.7 MHz high-frequency ultrasound generator (household humidifier, Sunbeam model 696) to generate micron-sized droplets. The mist was carried by an Ar flow at the rate of 1 standard liter per minute (SLPM) through two connected furnaces (first furnace = 275 °C, second furnace = 245 °C). The reaction was allowed to run for 2.5 h, and the product was collected in toluene-filled bubblers (Figure 1). The as-collected product was washed with methanol several times and redissolved in hexane for further characterization and use.

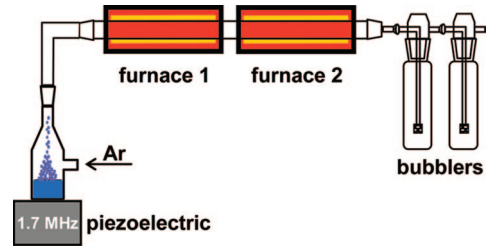

Figure 1. Schematic of Chemical Aerosol Flow Synthesis Apparatus.

For the synthesis of CdTeSe QDs emitting in the near-IR, the Se/Te molar ratio was increased from 6.0 to 30 and the furnace temperatures were 320 and 300 °C, respectively. For the synthesis of CdTeS QDs, TOPS (5 mmol) was added to the precursor solution instead of TOPSe. Overall reaction conditions were the same as in the synthesis of CdTeSe QDs emitting in the far-red.

Water-Soluble CdTeSe QDs via Ligand Exchange. The ligand exchange was similar to a previously reported procedure.[47] An aqueous solution (2.5 mL) containing aminoethanethiol (20 μM) was mixed with an equal volume of CdTeSe QD solution (optical density = 0.1 (~0.2 μM)) in hexane at room temperature in the dark for about 3 h. The phase transfer from the organic to the aqueous phase was easily checked by a hand-held UV lamp and confirmed by FT-IR (see the Supporting Information). After 3 h of stirring, the organic layer was discarded, and the aqueous QD layer was stored in the dark at 4 °C. Photo-oxidation of water-soluble CdTeSe QDs was carried out in an ambient atmosphere.

Characterization. UV−vis absorption and fluorescence spectra were taken using a HITACHI 3300 double monochromator UV−vis spectrophotometer and a Jobin Yvon Horiba FluoroMax-3 spectrofluorometer, respectively. The fluorescence quantum efficiency of the synthesized QDs was carefully measured using Rhodamine 6G as a standard. Transmission electron microscopy (TEM) images were taken with a JEOL 2010F with an acceleration voltage of 200 kV. X-ray diffraction (XRD) patterns were recorded on a Rigaku D-MAX diffractometer using Cu Kα radiation, and X-ray photoelectron spectroscopy (XPS) measurements were taken on a

(34) Nakamura, H.; Yamaguchi, Y.; Miyazaki, M.; Maeda, H.; Uehara, M.; Mulvaney, P. *Chem. Commun.* **2002**, 2844.
(35) Yen, B. K. H.; Stott, N. E.; Jensen, K. F.; Bawendi, M. G. *Adv. Mater.* **2003**, *15*, 1858.
(36) Wang, H.; Li, X.; Uehara, M.; Yamaguchi, Y.; Nakamura, H.; Miyazaki, M.; Shimizu, H.; Maeda, H. *Chem. Commun.* **2004**, 48.
(37) Yen, B. K. H.; Gunther, A.; Schmidt, M.; Jensen, K. F.; Bawendi, M. G. *Angew. Chem., Int. Ed.* **2005**, *44*, 5447.
(38) Didenko, Y.; Suslick, K. S. *J. Am. Chem. Soc.* **2005**, *127*, 12196.
(39) Yu, W. W.; Wang, A.; Peng, X. *Chem. Mater.* **2003**, *15*, 4300.
(40) Bao, H.; Gong, Y.; Li, Z.; Gao, M. *Chem. Mater.* **2004**, *16*, 3853.
(41) Tsay, J. M.; Pfluhoefft, M.; Bentolila, L. A.; Weiss, S. *J. Am. Chem. Soc.* **2004**, *126*, 1926.
(42) Kim, S.; Lim, Y. T.; Soltesz, E. G.; Grand, A. M. D.; Lee, J.; Nakayama, A.; Parker, J. A.; Mihaljevic, T.; Laurence, R. G.; Dor, D. M.; Cohn, L. H.; Bawendi, M. G.; Frangioni, J. V. *Nat. Biotechnol.* **2004**, *22*, 93.
(43) Zhang, Y.; He, J.; Wang, P.-N.; Chen, J.-Y.; Lu, Z.-J.; Lu, D.-R.; Guo, J.; Wang, C.-C.; Yang, W.-L. *J. Am. Chem. Soc.* **2006**, *128*, 13396.
(44) Ma, J.; Chen, J.-Y.; Guo, J.; Wang, C. C.; Yang, W. L.; Xu, L.; Wang, P. N. *Nanotechnology* **2006**, *17*, 2083.
(45) Ma, J.; Chen, J.-Y.; Guo, J.; Wang, C.-C.; Yang, W.-L.; Cheung, N.-H.; Wang, P.-N. *Nanotechnology* **2006**, *17*, 5875.
(46) Cho, S. J.; Maysinger, D.; Jain, M.; Roder, B.; Hackbarth, S.; Winnik, F. M. *Langmuir* **2007**, *23*, 1974.
(47) Wuister, S. F.; Swart, I.; van Driel, F.; Hickey, S. G.; de Mello Donegá, C. *Nano Lett.* **2003**, *3*, 503.

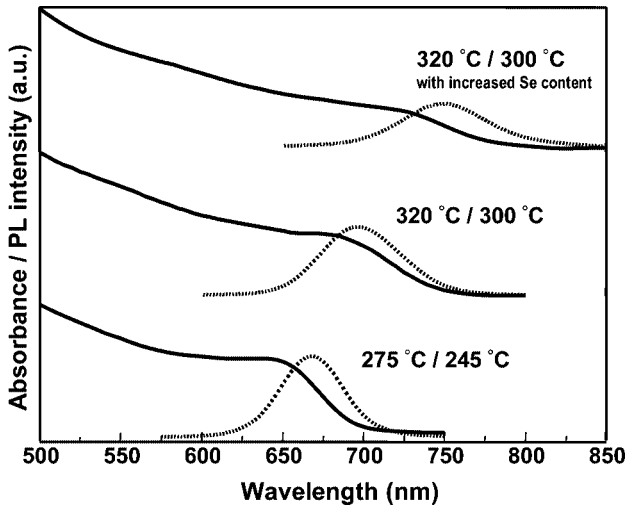

Figure 2. UV−vis absorption spectra (solid lines) and corresponding photoluminescence spectra (dashed lines) of CdTeSe QDs prepared at various dual furnace temperatures as indicated.

Kratos axis ultra imaging X-ray photoelectron spectrometer. Inductively coupled plasma mass spectroscopy (ICP-MS) was performed using a SCIEX ELAN DRCe system (PerkinElmer). Fourier transform infrared spectroscopy (FT-IR) was performed using a Nicolet Magna-IR 760 spectrometer. Nuclear magnetic resonance (NMR) experiments were carried out with a D_2O solution of CdTeSe QDs using a Varian Inova 500 (500 MHz) spectrometer.

Cellular Imaging with QDs. 1×10^5 to 1×10^6 SH-SY5Y (neuroblastoma) cells were cultured in Dulbecco's Modified Eagle Medium (DMEM) media containing 10% fetal bovine serum (FBS) at 37 °C under 5% CO_2 atmosphere. After the cells were stabilized, the aqueous CdTeSe QD solution was added to each well. After 1 day of incubation, the cells were washed with phosphate-buffered saline (PBS) several times to remove unbound QDs, and fresh cell media was reintroduced into the cells. Live SH-SY5Y (neuroblastoma) cells labeled with QDs were observed using a TCS SP2 confocal microscope (Leica Microsystems Inc.).

Results and Discussion

In the chemical aerosol flow synthesis (CAFS), a high-frequency ultrasound generator creates small droplets of precursor solution by nebulization, and the resulting mist is carried into a furnace with two heating zones: the first zone is used to remove the low boiling point solvent, toluene, leaving smaller, more concentrated droplets of a high boiling point solvent, octadecene,[38] and the second zone drives the chemical reactions that produce surfactant-stabilized nanoparticles, which are subsequently collected in bubblers filled with toluene.

The synthesized CdTeSe QDs emitting in the far-red region showed a band-edge emission at a maximum wavelength of 670 nm, and their quantum efficiency was found to be ~10%, as shown in Figure 2. The reaction is reproducible from a batch to a batch (variation in the absorption maximum is ± 5 nm). Rate of production of the QDs is ~20 mg/h under our reaction conditions; the production rate could be further boosted up by increasing precursor concentration and gas flow rate. The emission of the CdTeSe QDs could be further red-shifted to ~700 nm as the furnace temperatures increased to 320 and 300 °C,

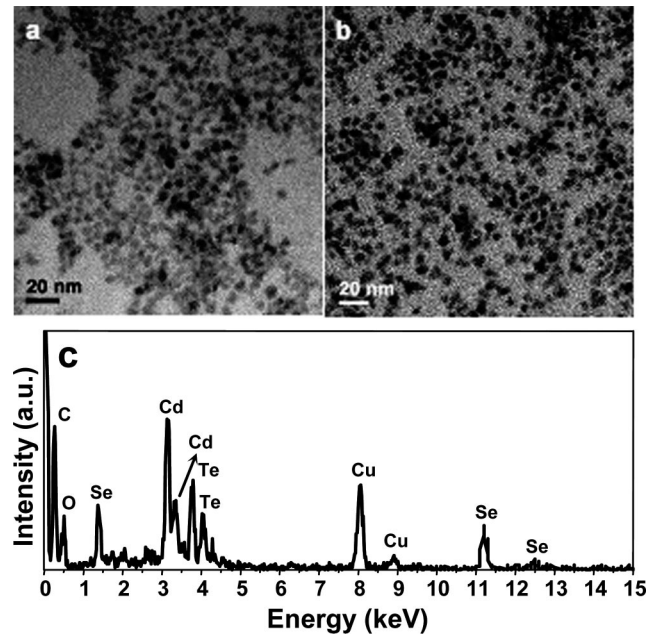

Figure 3. TEM images of CdTeSe QDs whose photoluminescence is in (a) the far-red (670 nm) and (b) the near-IR (750 nm), and (c) their TEM-EDS spectrum.

respectively, due to particle size increase. The photoluminescence of the CdTeSe QDs could be pushed even further into the near-IR region by increasing the amount of Se in the precursor solution at the same temperatures. The maximum emission of the CdTeSe QDs shifted up to ~750 nm, and the near-IR emitting QDs also showed a band-edge emission as observed in the far-red emitting QDs (Figure 2). Considering that CdTe QDs synthesized under the same conditions emit at ~670 nm, such a red-shift in photoluminescence of ternary CdTeSe QDs by 80 nm is dramatic. TEM images show that the average size of QDs was 5−6 nm, and the presence of three elements in the CdTeSe QDs was confirmed by energy-dispersive X-ray spectroscopy (EDS) analysis (Figure 3). While oleic acid-coated binary CdTe QDs typically show a hexagonal wurtzite structure,[39] XRD analysis shows that the ternary CdTeSe QDs have a cubic zinc blende structure with no significant peak shift to higher angles. The lack of peak shift is evidence for a thin CdSe shell instead of a CdTeSe alloy, which would have shown peak shifts in the XRD.[48] In addition, no separate diffraction peaks from CdSe QDs were observed, confirming the formation of ternary QDs (Figure 4a). Average particle size obtained using the Debye−Scherrer equation is 5.0 nm, which is in accord with TEM observation. The lattice constant of the CdTeSe QDs is found to be 6.46 Å, close to the lattice parameter of bulk CdTe (6.481 Å, JCPDS 15−0770). To gain more insight into the structural composition of the CdTeSe QDs, bulk elemental analysis (EA) and X-ray photoelectron spectroscopy (XPS) were conducted and compared. The characteristic peaks of Cd $3d_{5/2}$ (404.9 eV), Te $3d_{5/2}$ (572.0 eV), and Se 3d (54.3 eV) confirmed the existence of three elements in CdTeSe QDs (Figure 4b, see Figure S1 in the Supporting Information for detailed XPS spectra). The XPS data also allowed for the determination

(48) Seo, H.; Kim, S. W. *Chem. Mater.* **2007**, *19*, 2715.

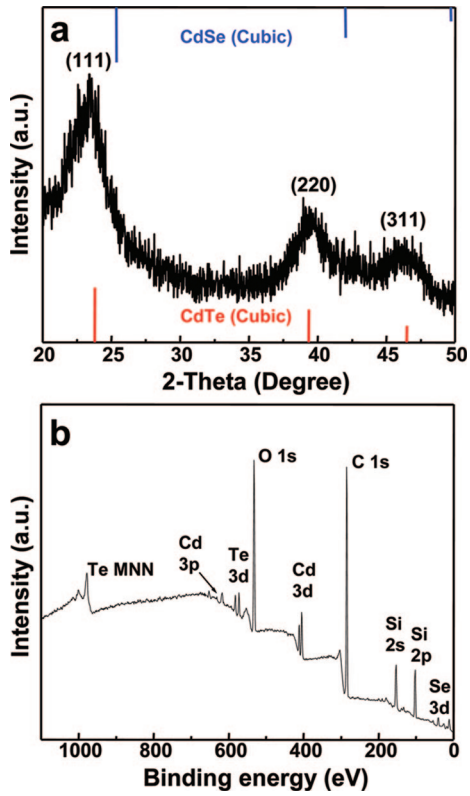

Figure 4. (a) XRD pattern of CdTeSe QDs (with blue and red lines indicating the JCPDS data for cubic CdSe and cubic CdTe, respectively). (b) XPS spectrum of CdTeSe QDs.

Table 1. Molar ratios of Te/Se and Te/S in CdTeSe and CdTeS QDs Determined by Bulk EA and XPS, Respectively

	Te/Se	
	EA	XPS
CdTeSe (670 nm)	3.35	0.79
CdTeSe (750 nm)	0.45	0.09

	Te/S	
	EA	XPS
CdTeS	1.38	1.32

of Te/Se ratio in the surface region of the CdTeSe QDs. The ratio of Te/Se determined by EA significantly decreases in the near-IR emitting CdTeSe QDs compared to the far-red emitting CdTeSe QDs. This indicates that the band gap of the ternary CdTeSe QDs is related to their composition (Te/Se molar ratio) as proposed by Nie and co-workers,[14] and the photoemission of the CdTeSe QDs was red-shifted by increasing the Se content in the precursor. Surprisingly, the Te/Se ratios determined by XPS were substantially smaller than those from the bulk EA (Table 1), which we attribute to the much higher relative reactivity of Te compared to Se under rapid nucleation and growth conditions.[14] Because XPS quantitative analysis is a surface sensitive technique (i.e., reveals surface rather than bulk composition), the bulk EA data combined with the XPS data demonstrate that CdTeSe QDs have a gradient structure with CdTe-rich core.

The CdTeS ternary QDs have several important improvements compared to CdTe or CdTeSe: improved quantum efficiency, effective surface passivation, and potentially, lower toxicity. Figure 5a gives the absorption and emission spectra of CdTeS ternary QDs. The photoemission of CdTeS QDs was observed near their band edge with a maximum emission at 651 nm, and their quantum efficiency was ~37% (see Figure 5b for photographic image). This substantial increase in the quantum efficiency of CdTeS QDs compared to CdTe QDs (quantum efficiency = ~20%) is attributed to the presence of a CdS outer shell in the ternary QDs. The CdS shell provides effective surface passivation due to the large bandgap and small lattice mismatch with CdTe core. TEM image shows that the prepared CdTeS QDs were monodisperse with an average size of ~5 nm, and their crystalline nature was revealed by the selected-area electron

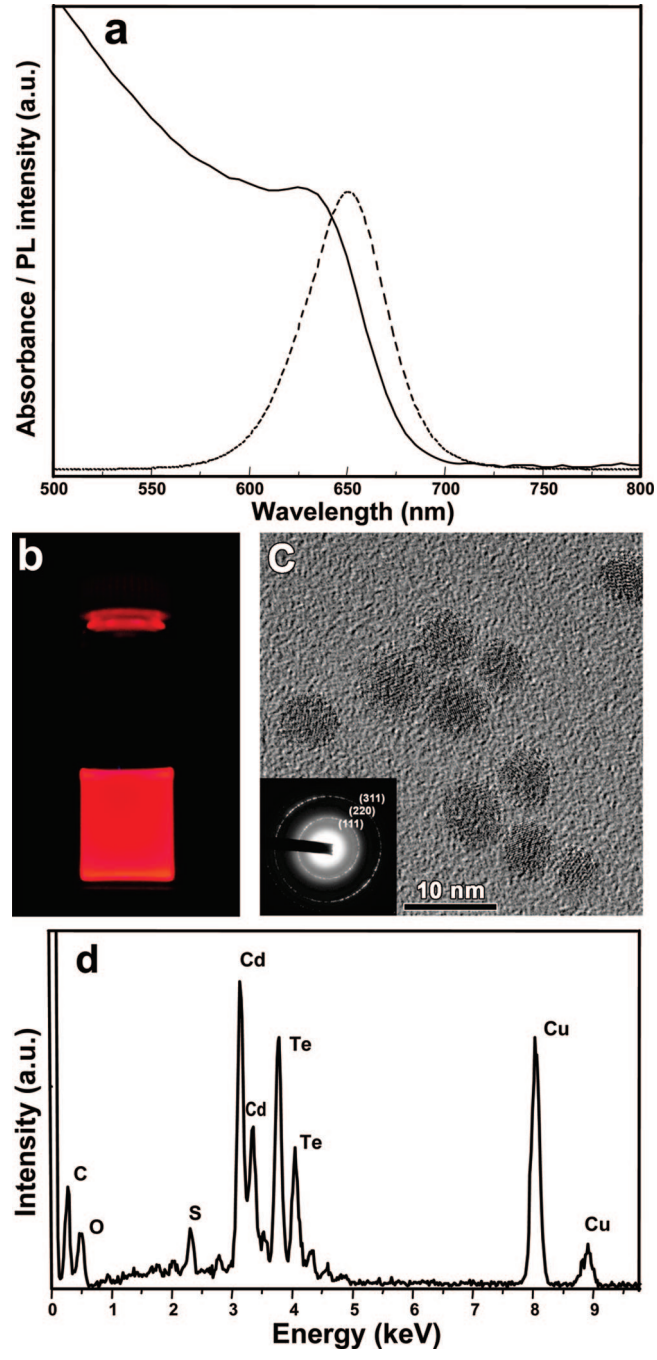

Figure 5. (a) Visible absorbance (solid line) and photoluminescence (dashed line) spectra, (b) photograph under a UV lamp, (c) TEM image, and (d) TEM-EDS spectrum of CdTeS QDs.

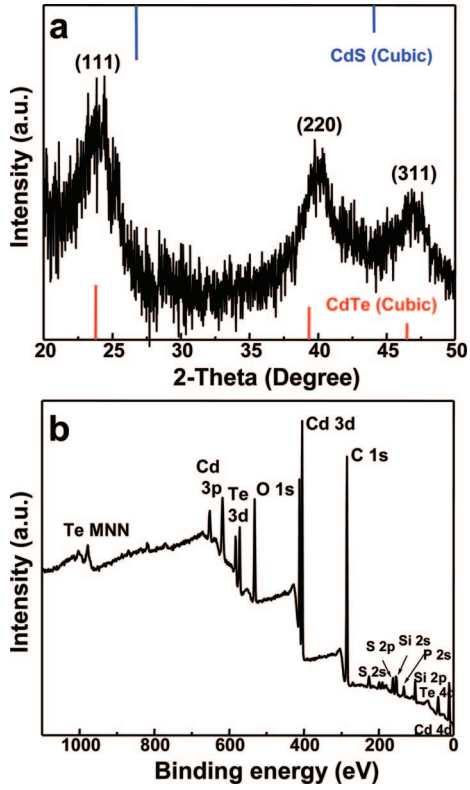

Figure 6. (a) XRD pattern of CdTeS QDs (with blue and red lines indicating the JCPDS data for cubic CdSe and cubic CdTe, respectively). (b) XPS spectrum of CdTeS QDs.

diffraction (SAED) pattern (Figure 5c). EDS clearly shows the presence of three elements in the CdTeS QDs (Figure 5d). XRD analysis of the CdTeS QDs reveals that the crystal structure of the QDs is cubic zinc blende with the diffraction peaks shifted toward slightly higher angles; i.e., the lattice constant of the CdTeS QDs is decreased to 6.30 Å as compared to that of bulk CdTe (this is consistent with either the formation of a thin CdS shell on CdTe or an alloyed CdTeS nanocrystal),[40] and XPS analysis also confirmed the formation of ternary CdTeS QDs (Figure 6 and Figure S2 in the Supporting Information for detailed XPS spectra). Average particle size obtained using the Debye−Scherrer equation is 4.2 nm, which is slightly smaller than the particle size determined by TEM observation (~5 nm) but within the error of measurement.

On the basis of all the characterization results (see Table 1 for EA and XPS quantitative analysis), we conclude that our CdTeS QDs have a gradient internal structure with a CdTe core and a CdS-rich surface, similar to the CdTeSe QDs; because of the contraction of the CdTe lattice constants, however, we cannot completely rule out the formation of alloyed CdTeS QDs. As the droplets of precursor solution experience heating in the furnace, CdTe QDs are formed much faster than CdS owing either to its lower solubility compared to CdS or to higher reactivity of Te than S;[49] we believe that these CdTe cores then act as a seed for shell growth. Such sequential growth of core CdTe particles with an overgrowth of a CdS shell produces CdTeS QDs with a

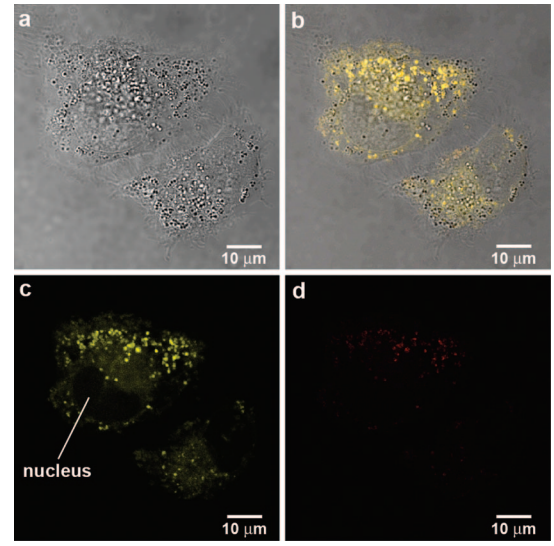

Figure 7. Confocal micrographs of SH-SY5Y (neuroblastoma) cells labeled with CdTeSe QDs after photo-oxidation: (a) bright-field image, (b) a merged image of bright field with total fluorescence, (c) yellow fluorescence with a 550−590 nm band-pass filter, (d) red fluorescence with a 610−670 nm band-pass filter.

higher quantum efficiency, as noted in the previous reports.[31,50,51] Although the quantum efficiency (Q.E.) of our gradient structured CdTeS QDs is lower than the core−shell structured CdTe/CdS QDs (Q.E. ≥ 50%), the CAFS technique has a potential advantage as a facile and robust one-pot synthetic route for high quality QDs because typical preparations of core−shell structured CdTe/CdS QDs involve multiple steps and requires extremely careful control of reaction parameters.

Water-soluble far-red emitting CdTeSe QDs were prepared by a simple phase transfer reaction,[47] and the ligand exchange from oleic acid to aminoethanethiol was confirmed by a FT-IR study (Figure S3 in the Supporting Information). We observed that the quantum efficiency of CdTeSe QDs after ligand exchange was substantially improved to ~25%, which is attributed to better surface passivation from the thiol ligands. The water-soluble CdTeSe QDs were then evaluated as a fluorescence labeling agent in live cell imaging applications. Confocal micrographs reveal that CdTeSe QDs were successfully endocytosed into SH-SY5Y (neuroblastoma) cells during incubation (Figure 7). To our surprise, most of the CdTeSe QDs were, however, yellow-light emitting, and only weak fluorescence was observed in the red region (see Figure S4 in the Supporting Information for additional confocal images). This observation suggests that the QDs were photo-oxidized during the imaging experiments; we note that the photoluminescence of binary CdTe QDs also undergoes a blue shift in living cells.[43–45]

To confirm that photo-oxidation was responsible for this blue shift, we directly exposed the water-soluble CdTeSe QDs to ambient light (i.e., standard fluorescent light fixtures) and air. Figure 8 shows the photoluminescence spectra of CdTeSe QDs over time during light exposure; the photolu-

(49) Liu, H.; Owen, J. S.; Alivisatos, A. P. *J. Am. Chem. Soc.* **2007**, *129*, 305.
(50) He, Y.; Lu, H.-T.; Sai, L.-M.; Lai, W.-Y.; Fan, Q.-L.; Wang, L.-H.; Huang, W. *J. Phys. Chem. B* **2006**, *110*, 13370.
(51) Jiang, W.; Singhal, A.; Zheng, J.; Wang, C.; Chan, W. C. W. *Chem. Mater.* **2006**, *18*, 4845.

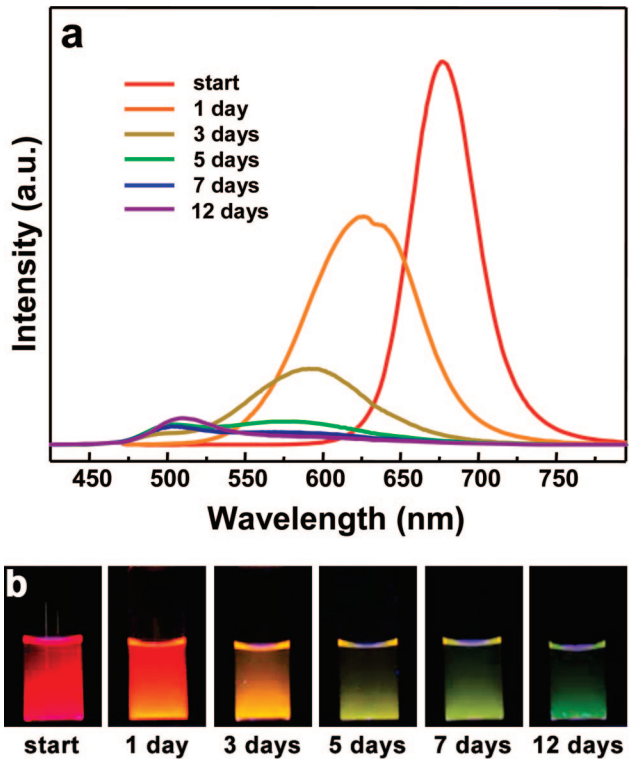

Figure 8. (a) Photoluminescence spectra of CdTeSe QDs during photo-oxidation under ambient conditions and (b) the corresponding photographs of fluorescence from a QD solution under a UV lamp. Blue shifts were not observed when identical suspensions were either exposed to air without light or exposed to light under N_2.

minescence of CdTeSe QDs was blue-shifted over the time, and the intensity dramatically decreased. This blue shift was not observed either in the absence of light under air or in the presence of light under N_2, confirming that the blue shift results from photo-oxidation (Figure S5 in the Supporting Information). Because the light source of the confocal microscope is much more intense than ambient light, the photo-oxidation of QDs within the cells proceeded much faster than that of QDs in aqueous solution under ambient light. The photo-oxidation was also confirmed by XPS analysis of the QDs obtained after light exposure (Figure S6 in the Supporting Information). The XPS spectra of Te 3d peaks from CdTeSe QDs before and after photo-oxidation reveal that two small peaks at binding energies of 576.0 and 586.4 eV appeared after photo-oxidation, which match the binding energy of TeO_2. TEM images before and after light exposure show that QDs had agglomerated during the photo-oxidation, which is attributed[52] to the loss of thiol ligands during the photo-oxidation process (Figure S7 in the Supporting Information). Such photochemical oxidation of thiol ligands was monitored by a NMR spectroscopy. The ratio of disulfides to thiols increased over time during light exposure, confirming the formation of disulfides during the photo-oxidation (Figure S8 in the Supporting Information). Our preliminary results reveal that the water-soluble CdTeS QDs (prepared by the same phase transfer reaction as used for water-soluble CdTeSe QDs) also exhibit photo-oxidation, which we attribute to the incomplete CdS coating in the CdTeS QDs.

Conclusions

Chemical aerosol flow synthesis has been further developed for the preparation of CdTeSe and CdTeS ternary QDs emitting in the red to near-IR regions. We are able to control the bandgap of the CdTeSe QDs by varying the composition ratio between Te and Se, and the quantum efficiency of CdTe was significantly increased by replacing Se with S in the precursor solution. The internal structure of the ternary QDs was revealed as a gradient structure with a CdTe-rich core. The ternary QDs could be rendered water-soluble via a simple phase transfer reaction, and the water-soluble CdTeSe QDs were evaluated as a fluorescence labeling agent in cellular imaging applications. A blue shift in the photoluminescence of CdTeSe QDs was observed both in living cells and in solution and shown to be due to photo-oxidation. This observation suggests that the effect of photo-oxidation and photobleaching as well as a way of preventing such effects (e.g., surface modification using silica[53–61] or polymer coatings[62,63]) must be considered prior to the use of CdTe QDs in cellular imaging applications.

Acknowledgment. We thank Dr. Yuri Didenko and Professor Yoo-Hun Suh for helpful discussions and gratefully acknowledge Dr. Richard Haasch, Dr. Yoonsoo Pang, and Ming Fang for helping with XPS, FT-IR, and NMR spectra acquisition, respectively. SH-SY5Y (neuroblastoma) cells were kindly provided by Prof. Yoo-Hun Suh. This work was supported by the National Science Foundation (CHE-03-15494). Research for this publication was carried out in the Center for Microanalysis of Materials, University of Illinois at Urbana−Champaign, which is partially supported by the U.S. Department of Energy under Grant DE-FG02-07ER46418.

Supporting Information Available: Detailed XPS spectra of CdTeSe and CdTeS QDs; FT-IR spectra of CdTeSe QDs before and after ligand exchange; more confocal micrographs of live cells labeled with CdTeSe QDs; and further characterization of CdTeSe QDs during photo-oxidation (PDF). This material is available free of charge via the Internet at http://pubs.acs.org.

CM800453T

(52) Aldana, J.; Wang, A.; Peng, X. *J. Am. Chem. Soc.* **2001**, *123*, 8844.
(53) Rogach, A. L.; Nagesha, D.; Ostrander, J. W.; Giersig, M.; Kotov, N. A. *Chem. Mater.* **2000**, *12*, 2676.
(54) Gerion, D.; Pinaud, F.; Williams, S. C.; Parak, W. J.; Zanchet, D.; Weiss, S.; Alivisatos, A. P. *J. Phys. Chem. B* **2001**, *105*, 8861.
(55) Chan, Y.; Zimmer, J. P.; Stroh, M.; Steckel, J. S.; Jain, R. K.; Bawendi, M. G. *Adv. Mater.* **2004**, *16*, 2092.
(56) Yang, Y.; Gao, M. Y. *Adv. Mater.* **2005**, *17*, 2354.
(57) Yi, D. K.; Selvan, S. T.; Lee, S. S.; Papaefthymiou, G. C.; Kundaliya, D.; Ying, J. Y. *J. Am. Chem. Soc.* **2005**, *127*, 4990.
(58) Bakalova, R.; Zhelev, Z.; Aoki, I.; Ohba, H.; Imai, Y.; Kanno, I. *Anal. Chem.* **2006**, *78*, 5925.
(59) Sathe, T. R.; Agrawal, A.; Nie, S. *Anal. Chem.* **2006**, *78*, 5627.
(60) Zhelev, Z.; Ohba, H.; Bakalova, R. *J. Am. Chem. Soc.* **2006**, *128*, 6324.
(61) Selvan, S. T.; Patra, P. K.; Ang, C. Y.; Ying, J. Y. *Angew. Chem., Int. Ed.* **2007**, *46*, 2448.
(62) Wang, D.; Rogach, A. L.; Caruso, F. *Nano Lett.* **2002**, *2*, 857.
(63) Kuang, M.; Wang, D.; Bao, H.; Gao, M.; Möhwald, H.; Jiang, M. *Adv. Mater.* **2005**, *17*, 267.